

To Offload or Not To Offload: Model-driven Comparison of Edge-native and On-device Processing

Nathan Ng

University of Massachusetts Amherst
Amherst, MA, USA
kwanhong@cs.umass.edu

David Irwin

University of Massachusetts Amherst
Amherst, MA, USA
irwin@ecs.umass.edu

Ananthram Swami

DEVCOM Army Research Laboratory
Adelphi, MD, USA
ananthram.swami.civ@army.mil

Don Towsley

University of Massachusetts Amherst
Amherst, MA, USA
towsley@cs.umass.edu

Prashant Shenoy

University of Massachusetts Amherst
Amherst, MA, USA
shenoy@cs.umass.edu

Abstract—Computational offloading is a promising approach for overcoming resource constraints on client devices by moving some or all of an application’s computations to remote servers. With the advent of specialized hardware accelerators, client devices are now able to perform fast local processing of specific tasks, such as machine learning inference, reducing the need for offloading computations. However, edge servers with accelerators also offer faster processing for offloaded tasks than was previously possible. In this paper, we present an analytic and experimental comparison of on-device processing and edge offloading for a range of accelerator, network, and application workload scenarios, with the goal of understanding when to use local on-device processing and when to offload computations. We present models that leverage analytical queuing results to capture the effects of dynamic factors such as the performance gap between the device and edge server, network variability, server load, and multi-tenancy on the edge server. We experimentally demonstrate the accuracy of our models for a range of hardware and application scenarios and show that our models achieve a mean absolute percentage error of 2.2% compared to observed latencies. We use our models to develop an adaptive resource manager for intelligent offloading and show its efficacy in the presence of variable network conditions and dynamic multi-tenant edge settings.

I. INTRODUCTION

Over the past decade, cloud computing has become the predominant approach for running online services in domains ranging from finance to entertainment. In recent years, a new class of online services has emerged that requires low-latency processing to meet end-user requirements. Examples of such applications include autonomous vehicles, interactive augmented and virtual reality (AR/VR), and human-in-the-loop machine learning inference [1]. Edge computing, which is a complementary approach to cloud computing, is a promising method to meet the needs of such latency-sensitive applications. Conventional wisdom has held that since edge resources are deployed at the edge of the network and are closer to end-users, edge-native processing can provide lower end-to-end latencies than cloud processing. However, recent research [2], [3] has shown that this conventional wisdom does not always hold—in

certain scenarios, edge processing can yield *worse* end-to-end latency despite its network latency advantage over the cloud. In particular, since edge clusters are resource-constrained relative to the cloud, research has shown resource bottlenecks can arise in the presence of time-varying workloads and increase the processing latency at the edge, negating its network latency advantage. Further, such bottlenecks can arise even at moderate levels of utilization, requiring careful resource management to maintain the benefits of edge-native processing [3].

A related trend is the emergence of *computational offloading* from local devices to remote resources such as those at the edge.¹ Computational offloading [4], [5] involves using nearby edge resources to take on some, or all, of an application’s processing demands. Such offloading is performed to overcome resource constraints on a local device by leveraging more abundant processing capacity at edge servers. Computational offloading is well-established in mobile computing where mobile devices, which are resource- or battery-constrained, offload local computations to edge servers [6]. In this case, local devices pay a so-called mobility penalty [7], which is the additional network latency to access edge servers, but then benefit from faster edge processing that outweighs this latency overhead. Offloading is also common for Internet-of-Things (IoT) devices that have limited on-board processing abilities and rely on remote processing to implement data processing tasks [8]. In these offloading scenarios, conventional wisdom holds that remote edge processing is faster than local processing despite the network overhead of accessing remote resources due to significant resource constraints at local devices.

With the advent of hardware accelerators in recent years, the conventional wisdom about the benefits of computational edge offloading for local devices needs to be rethought. For example, the rise of the so-called AI PC with onboard AI accelerators [9] has enabled local AI processing for many applications without a need for edge offloading. Similarly, mobile phones are

¹Computational offloading to the cloud is also common, but we focus on edge offloading in this paper.

equipped with neural accelerators [10] that enable efficient local inference, while IoT devices such as cameras have specialized accelerators to perform visual tasks (e.g., facial recognition) locally [11]. At the same time, edge servers can also be equipped with more powerful accelerators, such as GPUs, enabling offloaded tasks to also run more efficiently or faster than before. Thus, in the era of programmable accelerators, the question of whether to offload computations from local devices to the edge and when it is advantageous to do so needs to be reexamined. In particular, such a reexamination needs to address several questions. (i) Under what scenarios will local on-device processing using accelerators outperform edge offloading? (ii) Are there still scenarios where edge offloading has an advantage over local processing? (iii) What role does a fast (or slow) network between the device and the edge play in terms of whether to offload or not offload?

Motivated by the above questions, this paper takes an analytic model-driven approach to compare local and edge processing in the era of accelerators. Our hypothesis is that there is no a priori clear advantage of edge processing over on-device processing in the presence of accelerators, and that the choice of where to perform the processing depends on hardware, network, and workload characteristics. In developing our analytic models and validating this hypothesis, this paper makes the following contributions.

- We use queuing theory-based models to model the behavior of device and edge accelerators when processing requests for local on-device processing and edge offloading scenarios. Our modeling follows a two-level approach: it takes estimated service times obtained through profiling or other prediction techniques as input and embeds them into queuing models to obtain end-to-end response time predictions. Using these models, we develop closed-form analytic bounds to determine when one approach outperforms the other under different hardware, network, and workload scenarios. We also develop analytic models for comparing on-device processing to multi-tenant edge servers that serve multiple clients. Although our primary focus is on offloading, we also show how the models can be extended to account for device-edge collaborative (i.e., split) processing.
- We experimentally validate our analytic models and bounds using a variety of device and edge accelerators, network configurations, and workloads including deep neural networks (DNNs) and recurrent neural networks (RNNs). Our results show that our models are able to predict the performance behavior of on-device processing and edge offloading under various scenarios, achieving a mean absolute percentage error of 2.2%, with 91.5% of predictions falling within $\pm 5\%$ of the observed latency and 100% within $\pm 10\%$.
- We develop a dynamic resource manager that incorporates our models and demonstrate how they can be leveraged by this resource manager to adaptively switch between on-device and edge processing under time-varying workloads and under dynamic multi-tenancy scenarios. Our results show that it effectively adapts to changing network conditions and

fluctuating request rates at edge servers.

II. BACKGROUND

This section provides background on computational offloading, hardware accelerators, and on-device processing.

A. Cloud and Edge Offloading

Computational offloading is a well-known approach where client devices that are resource-constrained offload some or all of their application workload to a remote server. In the case of mobile devices such as AR/VR headsets, tablets, or smartphones, offloading can use nearby edge resources to perform latency-sensitive tasks [4], [5]. While such edge offloading involves a network hop to the edge server (also known as the mobility penalty [7]), subsequent processing at the edge is assumed to be much faster since edge resources are much less constrained than the devices. In the case of IoT devices or ML applications, offloading to the cloud is also common where the abundant processing capacity of the cloud platform is utilized for processing the application workload [12]. For example, large language model (LLM) inference uses GPU clusters in the cloud to answer user queries, while IoT devices use cloud storage and processing to perform analytic and data processing tasks.

In general, computational offloading offers benefits when local processing is constrained and the cost of incurring the additional network latency outweighs the benefits of accessing faster processing in the edge or the cloud.

B. Hardware Accelerators

In recent years, a wide range of programmable accelerators has been developed to accelerate a range of compute tasks, particularly machine learning compute. Such accelerators have been deployed on client devices, edge, and cloud servers, enabling faster processing of accelerated tasks at each tier. Table 1 depicts the characteristics of several commonly deployed device and edge accelerators, ranging from low-end to high-end options. Specifically, the Intel Movidius Myriad X Vision Processing Unit (VPU) is designed to accelerate vision-based applications [13]. Google Edge Tensor Processing Unit (TPU) optimizes ML inference with the TensorFlow Lite framework on the edge [14]. NVIDIA TX2, Orin Nano, and A2 are all tailored for AI workloads such as deep learning and computer vision [15], [16], [17]. For these specific workloads, programmable accelerators can provide substantial performance improvements, delivering server-like capabilities for some compute-intensive tasks even on low-end devices. With their small form factor and energy-efficient design, integrating accelerators into mobile devices has become increasingly common. For example, Apple devices include a Neural accelerator to accelerate machine learning tasks locally on the device [10]. With the presence of accelerators, fast on-device processing of tasks such as machine learning inference has become feasible without the need to resort to edge offloading. Meanwhile, edge servers can also be equipped with GPUs, which serve as general-purpose accelerators for a range of tasks, or special-purpose

TABLE I: Characteristics of common programmable accelerators.

Accelerator	Peak Power (W)	Memory	Cost	Target Workload
Intel Movidius Myriad X VPU	1 – 2.5	2.5 MB of SRAM	\$59	Computer vision and CNN inference
Google Edge TPU	2	8 MB of SRAM	\$75	ML Inference with TensorFlow Lite
NVIDIA Jetson TX2	15	8 GB of LPDDR4	\$399	AI and GPU workload
NVIDIA Jetson Orin Nano	15	8 GB of LPDDR5	\$499	AI and GPU workload
NVIDIA A2 GPU	60	16 GB of GDDR6	\$1399	AI and GPU workload

accelerators for specific tasks. This enables offloaded tasks to also be accelerated at the edge, making edge offloading useful for more compute-intensive tasks that a device may not be able to handle using local resources.

C. On-device Processing versus Edge Offloading

As noted above, the availability of accelerators on client devices has enabled on-device processing of many tasks without the need to offload those tasks to the edge or to the cloud. Since local processing does not incur any network hops, it will often be faster than remote processing which incurs an additional network latency. However, since edge servers can also be equipped with GPUs and other accelerators, in some compute-intensive scenarios, edge processing may still provide benefits over local processing on device accelerators. Thus, in the era of accelerators, local on-device processing may be faster in some scenarios, while offloading to edge accelerators may still be faster in other cases (after accounting for the network latency).

Even with extensive offline profiling of execution times on both the device and the edge, selecting the optimal execution strategy remains challenging due to dynamic real-world conditions. On the one hand, mobile devices are subject to network variability due to fluctuating wireless signal strength, interference, and congestion in shared communication channels. Since edge offloading requires transmitting input data to an edge server, network fluctuations introduce unpredictability in network delays, affecting its overall performance. Additionally, mobile devices running applications with prolonged operating durations, such as live object detection on captured video, may experience battery constraints. When operating in low-power mode, the system may underclock its processing units to conserve energy, resulting in extended execution times. On the other hand, edge servers are *multi-tenant* systems shared by multiple devices, which can result in interference across users and higher latencies. Since devices may independently decide when and whether to offload tasks, the edge server’s load can fluctuate dynamically based on the number and nature of tasks being offloaded at any given time. Compared to traditional cloud data centers, edge servers are often more resource-constrained, limiting their ability to elastically scale applications under resource pressure. Workload spikes in multi-tenant scenarios can increase queuing delays, significantly increasing end-to-end execution times. Moreover, edge servers are commonly multiplexed across different applications to maximize edge resources utilization. At the same time, GPUs and other programmable accelerators designed for edge servers often lack isolation mechanisms such as GPU virtualization that

are available in cloud-based GPUs [18], leading to performance interference between applications. As a result, execution times can become variable, making it challenging to determine whether to offload under dynamic workloads.

The above observations motivate the primary research question addressed in this paper: *Considering the hardware processing capabilities of the device and edge server, along with the workload characteristics and real-world dynamics, under what scenarios does one strategy outperform the other?* Specifically, does edge offloading still have a role to play when devices are equipped with on-board accelerators? How do workload dynamics, network dynamics, and edge multi-tenancy impact each strategy and their relative performance with respect to one another? To address this question, the next section develops analytic models to capture the end-to-end execution time for each on-device and edge processing, capturing the key factors that impact application performance.

III. MODEL-DRIVEN PERFORMANCE COMPARISON

In this section, we develop analytical queuing models for edge offloading and on-device processing, and derive closed-form expressions for their expected latencies to compare the two approaches and identify when one outperforms the other.

A. Analytic Queuing Models

Our analytical models are derived from queuing theory, a well-established mathematical tool for modeling response times experienced by requests in computing systems. Queuing theory has previously been used to model the performance of edge and cloud applications [2], [19], [20], and will serve as the foundation for analyzing edge offloading and on-device processing. As discussed below, we model the end-to-end latency of a request—the duration of time from when the task enters the first queue until it exits the system—for both edge offloading and on-device processing using queuing theory.

Edge offloading. To model the end-to-end request execution time using edge offloading, we need to model the times spent by the request both at the device and at the edge server. We do so by modeling the device and the edge as two separate queuing systems as shown in Figure 1a. We assume that the request arrives at the device and is then forwarded (“offloaded”) to the edge server over the network. We need to model any network queuing delays and the network transmission time of the request from the device to the server. Upon arrival at the edge server, the request is queued for processing and is subsequently scheduled for execution. Since accelerators employ data parallelism to process requests, we model the accelerator at the edge server as a parallel system that processes each request with a degree

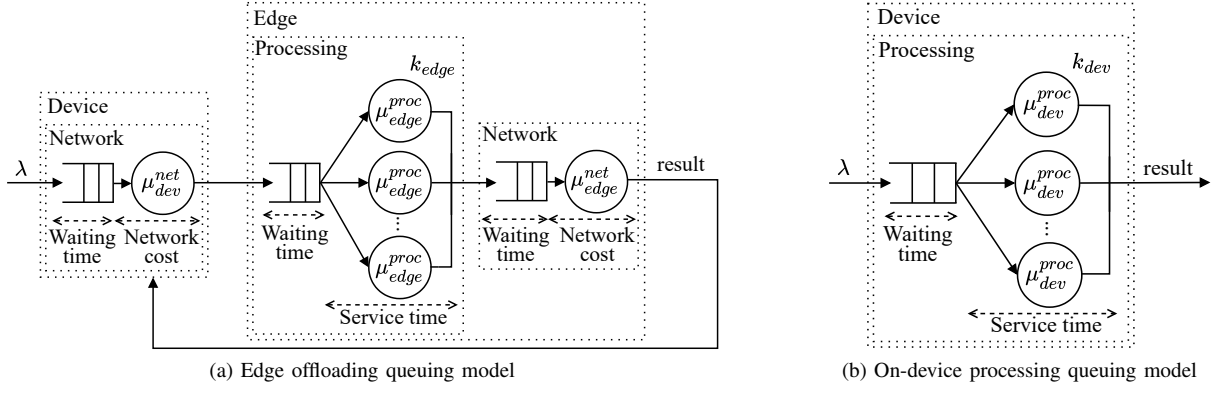


Fig. 1: Modeling request execution using (a) edge offloading and (b) on-device processing.

of parallelism k_{edge} . Once the request processing completes, the result is sent back to the device, which incurs network queuing delay and transmission latency on the reverse path.

On-device processing. Similar to edge offloading, we model on-device request processing as a queuing system shown in Figure 1b. Incoming requests generated by the device first enter a local device queue and are then scheduled onto one of the accelerator cores of the device where they are processed with a degree of parallelism k_{dev} . Upon completion of processing, the result is returned to the local application and the request exits the system. This model captures an application where a client device generates tasks, utilizes its accelerator cores for local execution, and sends the result to the application.

In queuing theory, the processing time of a request at each queue that it encounters consists of two key components: queuing delay (i.e., the time spent waiting in the queue) and service time (i.e., the time taken to execute the request on the accelerator). Let w_{dev}^{proc} , w_{edge}^{proc} , s_{dev} , and s_{edge} represent the wait times and request service times at the device and edge, respectively. Edge offloading additionally incurs network latency to transmit the request to the edge and the response back to the device, while on-device processing does not incur any network latency since all processing is local. Let w_{dev}^{net} and w_{edge}^{net} denote the respective network queuing delays on the device and the edge. Also, let n_{req} denote the network delay of sending a request from the device to the edge, and n_{res} be the network delay of sending a result from the edge to the device.

With the above notations, we now model the end-to-end latency of requests executed using each strategy:

$$T_{edge} = w_{dev}^{net} + n_{req} + w_{edge}^{proc} + s_{edge} + w_{edge}^{net} + n_{res} \quad (1)$$

and

$$T_{dev} = w_{dev}^{proc} + s_{dev} \quad (2)$$

where T_{edge} and T_{dev} denote the end-to-end request latency under edge offloading and on-device processing, respectively.

B. Deriving Service Times on Accelerators

Our analytic models require the service time of a workload as input to compute end-to-end response times. The service time reflects the computational demand on the target accelerator

and indicates how quickly a request is processed on a given platform. It can be obtained through empirical profiling or a deep learning model that predicts workload execution times on accelerators. For empirical profiling, many applications already support function-level performance logging or provide profiling hooks [21], which can be used to derive the service time of a request by analyzing the corresponding function's execution metrics. Alternatively, the workload can be profiled on the target hardware using benchmarking tools [22], [23]. In case of model-based prediction, a neural network can be trained to predict the service time of a model on a given target hardware. For example, prior work [24], [25], [26] estimates DNN inference latency by analyzing factors such as network structure and parameter size. For recurrent architectures such as Gated Recurrent Unit (GRU) networks and Long Short-Term Memory (LSTM) networks, existing latency estimation techniques [27], [28] incorporate factors such as temporal dependencies, hidden state dimensionality, and sequence unrolling behavior to accurately predict inference latency. While any of these prior techniques can be used with our analytic models, our experiments use a simple neural network model to predict the service times.

C. Deriving and Analyzing End-to-End Latency

In this section we compute the expected latency for edge offloading and on-device processing. Our analysis focuses on applications that require processing results on the device such as AR/VR applications. Note that our models can also be extended to capture the performance of applications that require results on the edge. In the following, we leverage classical queuing theory to fundamentally understand the conditions under which one strategy outperforms the other.

1) Comparing Edge Offload and On-Device Execution: We begin our analysis by examining the conditions under which edge offloading results in higher latency compared to on-device processing. For workloads that benefit from hardware acceleration such as those utilizing GPUs, processing times can be significantly reduced compared to processing on general-purpose CPUs. In the following discussion, we refer to such workloads as accelerator-driven workloads. While our analysis primarily focuses on DNN inference, the results generalize to

TABLE II: Notations used in analytic models.

Notation	Description
T_{dev}	End-to-end latency of on-device processing
T_{edge}	End-to-end latency of edge offloading
λ	Request arrival rate
B	Bandwidth of the device-to-edge network path
D_{req}, D_{res}	Payload sizes of request/result
$w_{dev}^{net}, w_{edge}^{net}$	Network wait time at the device/edge
n_{req}, n_{res}	Network transmission time of request/response
$\mu_{dev}^{net}, \mu_{edge}^{net}$	Service rate of device/edge NIC
k_{dev}, k_{edge}	Parallelism level of processors at device/edge
$w_{dev}^{proc}, w_{edge}^{proc}$	Processing wait time at the device/edge
s_{dev}, s_{edge}	Service time at the device/edge
$\mu_{dev}^{proc}, \mu_{edge}^{proc}$	Service rate of device/edge

other AI workloads as will be discussed in Section III-E. Table II summarizes the notation used in our models.

Lemma III.1. *For accelerator-driven workloads, edge offloading incurs a higher average end-to-end latency than on-device processing when*

$$s_{dev} - s_{edge} < \frac{\lambda}{\mu_{dev}^{net}(\mu_{dev}^{net} - \lambda)} + \frac{\lambda}{\mu_{edge}^{net}(\mu_{edge}^{net} - \lambda)} + \frac{D_{req} + D_{res}}{B} + \frac{1}{2} \left(\frac{1}{k_{edge}\mu_{edge}^{proc} - \lambda} - \frac{1}{k_{edge}\mu_{edge}^{proc}} \right) - \frac{1}{2} \left(\frac{1}{k_{dev}\mu_{dev}^{proc} - \lambda} - \frac{1}{k_{dev}\mu_{dev}^{proc}} \right) \quad (3)$$

Proof. Edge offloading will offer a worse latency than on-device processing when $T_{device} < T_{edge}$. That is

$$w_{dev}^{proc} + s_{dev} < w_{dev}^{net} + n_{req} + w_{edge}^{proc} + s_{edge} + w_{edge}^{net} + n_{res} \quad (4)$$

Let D_{req} and D_{res} denote the task and result payload size, respectively. Further, let B denote the bandwidth of the device-to-edge network path. The above inequality reduces to

$$s_{dev} - s_{edge} < w_{dev}^{net} + w_{edge}^{net} + \frac{D_{req}}{B} + \frac{D_{res}}{B} + w_{edge}^{proc} - w_{dev}^{proc} \quad (5)$$

As shown in [29], DNN inference on programmable accelerators often exhibits deterministic service times (denoted as D), as the number of operations per request remains constant. Since typical accelerators have a small degree of parallelism k [30], the queuing system can be modeled as an $M/D/k/FCFS$ system, where request arrivals follow a Poisson process. While no closed-form solution exists for the expected wait time in such a system, a common approximation is to aggregate the service rate across the degree of parallelism k [31], [32]. This reduces the model to an $M/D/1/FCFS$ system with aggregated service rate $k\mu$. Its expected wait time can be derived from the Pollaczek-Khinchin (P-K) formula [33], [19] and is given by

$$E[w_{M/D/1}] = \frac{1}{2} \left(\frac{1}{k\mu - \lambda} - \frac{1}{k\mu} \right) \quad (6)$$

On the other hand, network interfaces with a single controller can be modeled as $M/M/1/FCFS$ systems with expected wait times given by

$$E[w_{M/M/1}] = \frac{1}{\mu - \lambda} - \frac{1}{\mu} \quad (7)$$

Let k_{dev} and k_{edge} denote the degree of parallelism seen at the accelerator on the device and the edge respectively. Applying these two results to (5), we get

$$s_{dev} - s_{edge} < \frac{1}{\mu_{dev}^{net} - \lambda_{dev}^{net}} - \frac{1}{\mu_{dev}^{net}} + \frac{1}{\mu_{edge}^{net} - \lambda_{edge}^{net}} - \frac{1}{\mu_{edge}^{net}} + \frac{D_{req} + D_{res}}{B} + \frac{1}{2} \left(\frac{1}{k_{edge}\mu_{edge}^{proc} - \lambda_{edge}^{proc}} - \frac{1}{k_{edge}\mu_{edge}^{proc}} \right) - \frac{1}{2} \left(\frac{1}{k_{dev}\mu_{dev}^{proc} - \lambda_{dev}^{proc}} - \frac{1}{k_{dev}\mu_{dev}^{proc}} \right) \quad (8)$$

Offloading is only required when a request arrives, which gives us $\lambda_{dev}^{net} = \lambda$. For a queuing system to be stable, throughput (i.e., task completion rate) must equal the task arrival rate λ under steady-state conditions. When tasks are offloaded to an edge server, results are transmitted to the device only upon task completion, which yields $\lambda_{edge}^{net} = \lambda$. The first two terms involving μ_{dev}^{net} on the RHS can be written as

$$\frac{1}{\mu_{dev}^{net} - \lambda_{dev}^{net}} - \frac{1}{\mu_{dev}^{net}} = \frac{\lambda}{\mu_{dev}^{net}(\mu_{dev}^{net} - \lambda)} \quad (9)$$

whereas the second two terms involving λ_{edge}^{net} can be written as

$$\frac{1}{\mu_{edge}^{net} - \lambda_{edge}^{net}} - \frac{1}{\mu_{edge}^{net}} = \frac{\lambda}{\mu_{edge}^{net}(\mu_{edge}^{net} - \lambda)} \quad (10)$$

Moreover, regardless of the execution strategy, the application sees the same arrival rate, i.e., $\lambda_{dev}^{proc} = \lambda_{edge}^{proc} = \lambda$. Substituting the above into (8), we obtain

$$s_{dev} - s_{edge} < \frac{\lambda}{\mu_{dev}^{net}(\mu_{dev}^{net} - \lambda)} + \frac{\lambda}{\mu_{edge}^{net}(\mu_{edge}^{net} - \lambda)} + \frac{D_{req} + D_{res}}{B} + \frac{1}{2} \left(\frac{1}{k_{edge}\mu_{edge}^{proc} - \lambda} - \frac{1}{k_{edge}\mu_{edge}^{proc}} \right) - \frac{1}{2} \left(\frac{1}{k_{dev}\mu_{dev}^{proc} - \lambda} - \frac{1}{k_{dev}\mu_{dev}^{proc}} \right) \quad (11)$$

which completes the proof. \square

The above result implies the following two remarks.

Remark III.1. *On-device processing is likely to outperform edge offloading for workloads with lower computational demand.*

Explanation. Service time, which is the time spent processing a request on an accelerator, is determined by the computational

demand of the workload divided by the processing capacity of the hardware. For any given hardware configuration, requests with lighter demand have to be processed much faster at the edge to overcome the network penalty for edge offloading to be faster than on-device processing. For requests with lower computational demands, the difference in average service times $s_{dev} - s_{edge}$ shrinks proportionally due to the disparity in processing capacities between the device and the edge as the workload computational demand decreases. Further, since the service rate is the inverse of service times in queuing theory (i.e., $s = 1/\mu$), the terms with μ_{dev}^{proc} and μ_{edge}^{proc} on the right hand side of the inequality in (3) will also become smaller since μ increases for lighter requests. The terms representing the network overheads remain unchanged since they depend on request size rather than the processing demand of the request. As a result, the inequality in (3) is more likely to hold true for requests with lighter processing demand. \square

Remark III.2. *On-device processing is likely to outperform edge offloading on slower networks or when workloads have larger request or result payloads.*

Explanation. The term $\frac{D_{req} + D_{res}}{B}$ in (3) increases when either the network bandwidth B decreases or the request and result sizes D_{req} and D_{res} become larger, thereby increasing the right hand side of the inequality. In addition, longer transmission times reduce the service rates of the NIC at the device and edge (μ_{dev}^{net} and μ_{edge}^{net}), further increasing the RHS. As a result, the inequality is more likely to hold for slower networks or tasks with higher network overheads, making on-device processing faster than edge offloading. \square

Practical takeaways. Lemma III.1 establishes a bound on the average service time difference between device and edge for edge offloading to be more effective. The bound and the resulting inequality depends on several factors: (i) relative processing speeds of the device and edge, denoted by s_{dev} , s_{edge} (and also the corresponding service rates μ_{dev} and μ_{edge}), (ii) network speed, (iii) overall workload denoted by request rate λ , (iv) network transmission overheads. In general, for any specific workload, the edge processing capacity must be larger than the device processing capacity by a factor that overcomes the network penalty of offloading the workload; otherwise, on-device processing becomes preferable to offloading.

Moreover, the request rate λ impacts offloading decisions in two competing ways. First, as λ increases, both the edge and the device experience longer queuing delays, with the edge queue growing more slowly due to its faster processing speed. Consequently, the benefits of offloading improve under high load. However, under slow network conditions or for applications with large payloads, a high λ increases the network queuing delay (first two terms of the right side of the inequality) and may lead to network congestion, making on-device processing preferable. Thus, the optimal strategy depends on the workload's payload size relative to both network bandwidth and the edge-device performance gap.

Remark III.1 shows how the computational demand of the workload influences the execution strategy. For workloads with

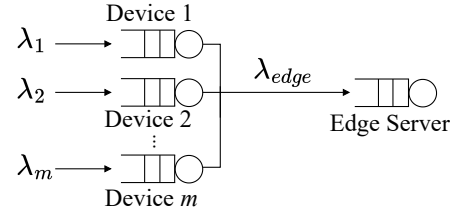


Fig. 2: m devices offloading requests to an edge server.

higher computational demand, edge offloading is more likely to outperform on-device processing, as the edge's processing speed advantage becomes larger. Conversely, for workloads with lower computational demand, on-device processing is more efficient as the performance advantage of edge processing is likely outweighed by the associated network costs. Remark III.2 demonstrates how network delays affect the efficiency of edge offloading. With smaller network bandwidth or larger request/result payloads, both the network queuing delay and transmission time increase. As a result, edge offloading becomes less efficient, while on-device processing is unaffected since it does not rely on network resources.

Extending to collaborative processing. Collaborative (i.e., split) processing involves partially processing requests locally on the client's device before offloading them to a remote edge server to minimize the amount of data sent over the network [34], [35], [36], [12], [26], [37], [38]. To compute the end-to-end response time of such a strategy, we combine our analytic models for on-device processing and edge offloading into a tandem queuing network that accounts for both the partial local computation and the subsequent transmission and processing delays at the edge server. Specifically, a request first enters the components modeled in Figure 1b and is partially processed with a service time s'_{dev} representing the partial local processing time. Then, the intermediate output of size D_{inter} passes through the components modeled in Figure 1a, with a network transmission time of D_{inter}/B and a service time s'_{edge} representing the remaining computation time on the edge. This combined model can then be used to estimate performance and inform decision-making when selecting between local, edge, or collaborative processing strategies.

D. Impact of Multi-Tenancy

While the analysis in Lemma III.1 implicitly assumes an edge server that is dedicated to a client device, in practice, edge servers will be multiplexed across multiple client devices and service multiple applications that offload their work. Hence, we extend our model-driven comparison to multi-tenancy scenarios.

Modeling edge application multiplexing. In the case where each edge server is dedicated to a single client device, the workload (i.e., the request arrival rate) at the edge and the device λ_{dev}^{proc} and λ_{edge}^{proc} are identical. However, when an edge server is multiplexed across m devices, its workload will be the sum of the individual device workloads under the offloading case, as shown in Figure 2. This higher workload will increase

the queuing delays at the edge and may cause the end-to-end offloading latency to exceed the on-device processing latency.

Since the request arrivals at each client device are governed by independent Poisson process, and the composition of independent Poisson processes results in a new Poisson process [39], it follows that the aggregate edge workload is also Poisson with an arrival rate λ_{edge} that is the sum of the device workload. That is, $\lambda_{edge} = \sum_{i=0}^m \lambda_i$, where λ_i denotes the workload at the i -th device.

We assume that the multiplexed applications have different service time demands, and the aggregate service time distribution seen at the edge will be arbitrary. For this case, we model each system as an $M/G/1$ system, where M denotes Poisson arrivals and G denotes the general (arbitrary) service time distribution seen at the device and the edge. This extension captures the potentially large variability in service times across applications in multi-tenant environments. If s_i denotes the average service time of requests of device i when processed at the edge, then s_{edge} is the weighted average of these service times. That is, $s_{edge} = \sum_i \frac{\lambda_i}{\lambda_{edge}} s_i$ and the effective service rate of the edge $\mu_{edge} = 1/s_{edge}$. Then the aggregate utilization of the edge server ρ_{edge} is $\rho_{edge} = \lambda_{edge}/\mu_{edge}^{proc}$. This leads us to the following lemma for the multi-tenant case.

Lemma III.2. *For multi-tenant edge servers, the average end-to-end latency of edge offloading is higher than on-device processing when*

$$\begin{aligned} s_{dev} - s_{edge} &< \frac{\lambda_{dev}}{\mu_{dev}^{net}(\mu_{dev}^{net} - \lambda_{dev})} \\ &+ \frac{\lambda_{edge}}{\mu_{edge}^{net}(\mu_{edge}^{net} - \lambda_{edge})} + \frac{D_{req} + D_{res}}{B} \\ &+ \frac{\rho_{edge} + \lambda_{edge} k_{edge} \mu_{edge}^{proc} \text{Var}[s_{edge}]}{2(k_{edge} \mu_{edge}^{proc} - \lambda_{edge})} \\ &- \frac{1}{2} \left(\frac{1}{k_{dev} \mu_{dev}^{proc} - \lambda_{dev}} - \frac{1}{k_{dev} \mu_{dev}^{proc}} \right) \end{aligned} \quad (12)$$

Proof. The expected wait time of $M/G/1/FCFS$ systems is well-known and is given by the Pollaczek-Khinchin (P-K) formula [33], [19]

$$E[w] = \frac{\rho + \lambda \mu \text{Var}[s]}{2(\mu - \lambda)} \quad (13)$$

Substituting (13) for w_{edge}^{proc} , (6) for w_{dev}^{proc} , and (7) for w_{dev}^{net} and w_{edge}^{net} into (5) completes the proof. \square

Practical takeaways. The expected wait time in $M/G/1/FCFS$ systems is heavily affected by the variance in service times, meaning that co-located applications with highly variable service demands can significantly increase queuing delays. It is therefore important for application designers to consider service time variability when assigning applications to edge servers. Grouping applications with similar processing demands can help reduce overall variability, thereby minimizing queuing delays and improving edge offloading performance. Further, the above analysis assumes that isolation features such

as GPU virtualization, which are available on server-grade GPUs, *are not available on edge accelerators*. If such features were available, each device could be assigned to an isolated virtual GPU on the edge. In this special case, the offloading situation is reduced to a situation similar to that considered in Sec III-C1 where each virtual GPU presents $\frac{1}{m}$ -th of the capacity to each device. However, many edge accelerators lack such features, resulting in a shared accelerator that services a combined workload.

E. Discussion

Generalizing to other accelerator-driven workloads. While the above analysis focuses on DNN workloads with deterministic service times modeled using an $M/D/1$ system, our modeling framework can be extended to other workloads with different service time characteristics by incorporating appropriate queuing results. For example, workloads with recurrent architectures such as GRUs and LSTMs often process variable-length inputs with service times that vary with the input sequence length. Similarly, early-exit DNNs allow requests to exit at different layers based on confidence thresholds, which results in variable service times. To capture such variability, our framework can adopt an $M/M/1$ queuing system where service times follow an exponential distribution with the expected wait time shown in (7). By selecting the appropriate queuing model, our framework can adapt to diverse workloads and provide accurate response time estimates as will be shown in Section IV-D. Currently, our framework does not account for workloads that violate the FCFS assumption, such as Large Language Model (LLM) inference with continuous batching where requests are dynamically batched, and extending the models to capture such behavior is a subject of future work.

Model limitations. Our analysis assumes request arrivals follow a Poisson process and are independent, which may not hold under bursty arrivals. To address this, our models can adopt a $G/G/1$ system, which accommodates arbitrary arrival and service time distributions. Although no closed-form solution exists for the expected wait time in this setting, Marshall et al. [40] provide an upper bound

$$E[w_{G/G/1}] \leq \frac{\lambda(\sigma_a^2 + \sigma_s^2)}{2(1 - \rho)} \quad (14)$$

where σ_a and σ_s are the variances for the interarrival and service distributions respectively. Additionally, the queuing results used in our analysis assume that each hardware queue has infinite capacity. For scenarios with bounded queue sizes, we can incorporate results for finite-buffer queuing systems [19] to model the impact of such capacity constraints.

IV. MODEL VALIDATION

In this section, we empirically evaluate how the key factors modeled in our analytic framework affect the performance of the two execution approaches and demonstrate that our models can accurately predict the response times across a wide range of configurations.

A. Experimental Setup

Workloads. We validate our model’s ability to capture the impact of workload characteristics using a diverse set of workloads, including DNN-based models as well as recurrent models. For DNN workloads, we focus on cognitive assistant applications involving image classification and object detection. Specifically, we use three widely deployed DNN architectures, namely MobileNet, Inception, and YOLO, each with distinct computational demands and input sizes as shown below:

Model	Input Shape	Params (M)	FLOPs (G)
MobileNetV2	[224, 224, 3]	3.5	0.6
InceptionV4	[299, 299, 3]	42.7	6.3
YOLOv8n	[640, 640, 3]	3.2	8.7

All inference requests are executed using TensorFlow 2.13.0 across the evaluated hardware. We use frames extracted from a 720p dash cam video as input to the models, with each frame processed either locally on the device or offloaded to the edge. Since application workloads are often dynamic (e.g., triggered by motion detection), we implement a workload generator that selects video frames and generates requests following a Poisson process, which runs on a separate machine to avoid performance interference with the device during evaluation. For recurrent models, we focus on personal voice assistant applications involving sentiment classification of conversational utterances. We validate our models using two types of recurrent neural networks: a GRU model with lower computational demand and a more compute-intensive LSTM model, with their architectural specifications summarized below:

Model	Embedding Dim	# Layers \times Units	Activation
GRU	512	2×512	Sigmoid
LSTM	1024	3×1024	Sigmoid

Both models are implemented using TensorFlow’s Keras API. To simulate real-world user inputs, we use the Amazon Alexa Topical Chat dataset [41], a knowledge-grounded human-to-human conversation dataset consisting of spoken-style dialogues with an average utterance length of 19 tokens.

Hardware. We use a diverse set of hardware platforms to reflect real-world deployment scenarios. For client devices with accelerators, we use the NVIDIA Jetson TX2 and Jetson Orin Nano, two commonly deployed platforms in IoT applications, with the TX2 being an earlier model and the Orin Nano offering better performance. For edge servers, we use a Dell PowerEdge R630 equipped with an NVIDIA A2 GPU, a 40-core Intel Xeon E5-2660v3 CPU, and 256GB RAM. We also use a server with an NVIDIA RTX 4070 GPU, 8-Core AMD Ryzen 7 5700X CPU, and 32GB RAM. Both edge servers are connected to a 1 Gbps network. These platforms span a wide performance range, from 1.3 TFLOPS (TX2) to 2.6 TFLOPS (Orin Nano), 4.5 TFLOPS (A2), and up to 29.1 TFLOPS (RTX 4070) in peak FP16 throughput. For each accelerator, the effective degree of parallelism k depends on both the number of cores and the workload’s processing and memory demands, and is not directly observable. To estimate k , we empirically measure how

response time varies with request rate for each workload and identify a value of k that best captures the observed scaling behavior. All platforms run Ubuntu 18.04, and we use the Linux Traffic Control (TC) subsystem to emulate different network bandwidths.

B. Parameter Estimation

Our model requires several parameters to compute the end-to-end response times. We now describe how these parameters are obtained in our evaluation and outline other practical methods for estimating them.

Estimating average service times. Our system estimates workload service times through empirical profiling and a neural network-based prediction approach. We estimate service times for DNN workloads by monitoring inference durations using the NVIDIA System Management Interface (nvidia-smi) tool [23], which reports per-process execution times on the accelerator. For GRU and LSTM workloads, we profile request latencies on a representative input set distinct from the test set and use the average latency from this profiling as the service time of the model. This profiling data is used for our edge-offloading and on-device processing experiments. For collaborative processing, a neural network is trained using profiling data to predict service time based on prior work discussed in Section III-B. Such a neural network approach avoids the extensive profiling overhead of all possible split configurations by predicting partial execution service times.

Estimating average network delays. Estimating transmission delay requires knowledge of the available network bandwidth, which we continuously measure in real-time using iperf [42]. In addition to queuing and transmission delays captured by our models, network delays also include propagation and processing delays. Since we assume that requests are offloaded to a nearby edge server, the propagation delay (caused by signals traveling at the speed of light) is minimal and thus excluded from our models. Processing delay can be estimated by measuring the round-trip time of small probe packets, and is excluded from our models due to its negligible impact on overall latency.

Estimating system utilization. The system utilization ρ is calculated as the ratio of the arrival rate λ to the service rate μ of the system. The arrival rate λ can be estimated by applying a sliding window over incoming request timestamps. The service rate μ can be estimated from system logs based on the number of completed requests within a given time interval.

C. Impact of Workload Characteristics

Our first experiment investigates how workload characteristics influence offloading decisions using three DNN workloads with distinct profiles: 1) MobileNetV2 (low compute, small payload); 2) InceptionV4 (high compute, moderate payload); and 3) YOLOv8n (high compute, large payload). We compare on-device processing on TX2 and Orin Nano against offloading to an A2 GPU using a request rate of 2 requests per second (RPS) and a network speed of 5 Mbps. For each device, we test all available GPU frequency settings to emulate different device conditions.

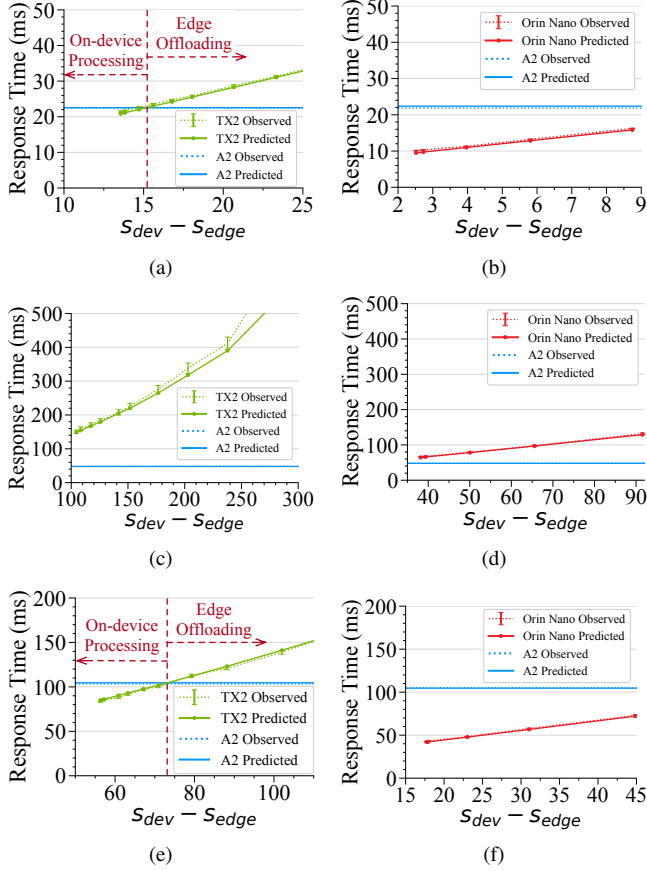


Fig. 3: Latency comparison across workloads at 5 Mbps network speed and 2 RPS. (a-b) MobileNetV2, (c-d) InceptionV4, and (e-f) YOLOv8n. Left: TX2 vs A2; Right: Orin Nano vs A2.

Figure 3 compares the average latency of on-device processing and edge offloading across workloads, devices, and GPU frequency levels. Figures 3a and 3b show that for MobileNetV2, local processing on both devices outperform offloading: TX2 achieves lower latency in its three highest frequency modes, while Orin Nano consistently outperforms offloading across all frequency levels. The trend reverses for InceptionV4 as shown in Figures 3c and 3d, where offloading provides lower average latency across all device configurations. Lastly, Figures 3e and 3f shows the results for YOLOv8n. In contrast to the results for InceptionV4, TX2 outperforms offloading in its top six performance modes despite YOLOv8n’s high compute demand, while Orin Nano achieves lower average latency than offloading across all performance modes. We observe similar results when offloading to RTX4070 and omit the details here due to space constraints. In all cases, the model predictions closely match the observed response times for both approaches, achieving a mean absolute percentage error of 2.2%, with 91.5% of predictions falling within $\pm 5\%$ of the observed latency and 100% within $\pm 10\%$, proving the accuracy of our models.

Collectively, these empirical results align with the qualitative

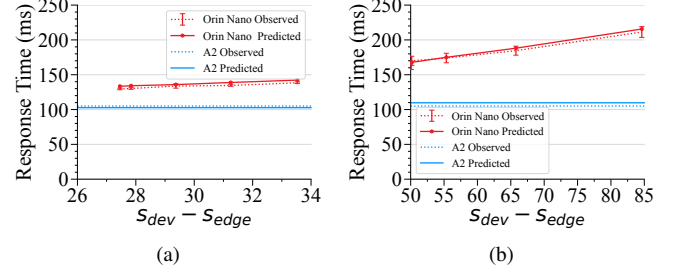


Fig. 4: Latency comparison across execution strategies for (a) GRU model and (b) LSTM model at 3 RPS under 10 Mbps.

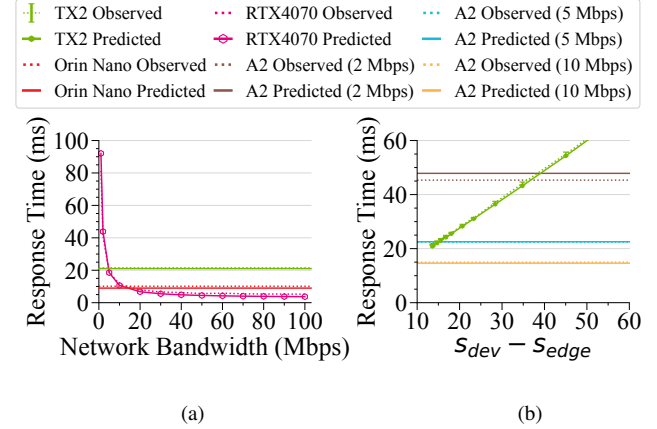


Fig. 5: Latency comparison across execution strategies for MobileNetV2 at 2 RPS with varying network bandwidth: (a) RTX4070 as the edge server, (b) A2 as the edge server.

observations stated in Remark III.1 and Remark III.2. While the performance ratio between edge and device is fixed, the absolute advantage of offloading scales with the workload’s demands. For workloads with low computational demand (MobileNetV2), the edge’s relative speed advantage results in only small absolute gains that can be overshadowed by network delays of offloading. However, for compute-intensive workloads (InceptionV4), the same performance ratio yields substantially larger absolute improvements that outweigh the network delays. Moreover, workloads with large message payloads (YOLOv8n) favor on-device processing because it does not involve any network components and thus avoids any network delay.

Key takeaway. Offloading provides lower latency when the edge’s absolute performance gain exceeds the associated network delay. Our models accurately predict the latency for both strategies with a mean absolute percentage error of 2.2%.

D. Impact of Complex Deep Learning Models

In addition to the DNN workloads, our model also accurately captures the latency behavior of more complex deep learning workloads. Figure 4 compares the average latency of on-device processing on the Orin Nano against offloading to A2 for two recurrent models: GRU and LSTM, under a moderate load of 3 RPS. Since service times vary with input length in these

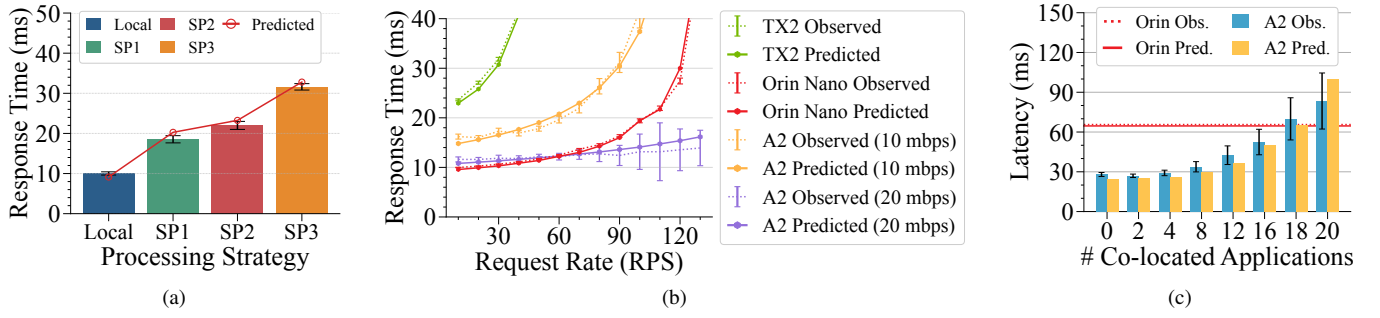


Fig. 6: Latency comparisons across (a) different collaborative processing configurations, (b) request rates under 10 Mbps and 20 Mbps networks, and (c) numbers of co-located applications.

models, we incorporate the $M/M/1$ queuing model into our analysis to account for this variability in latency prediction.

Figure 4a shows that even for the lightweight GRU model, offloading offers lower latency due to the small input utterance length (on average less than 100 bytes), which incurs minimal network delay. Figure 4b shows that as the model complexity increases, the absolute performance gain of offloading increases, leading to a greater latency reduction. In both cases, our model predictions closely match the observed latencies.

Key takeaway. Our models generalize to complex deep learning workloads beyond DNN inference by integrating appropriate queuing models.

E. Impact of Network Conditions

Figure 5 shows how network speed affects the effectiveness of each execution strategy. Figure 5a compares the latency of on-device processing on TX2 and Orin Nano with edge offloading to RTX4070 under varying network speeds. For both devices, we observe a performance crossover point where offloading becomes faster than on-device processing. The location of the crossover depends on both network bandwidth and the performance gap between the device and the edge. For the lower-performance TX2, offloading becomes advantageous at 5 Mbps, while the faster Orin Nano requires a higher bandwidth (15 Mbps) for offloading to be beneficial.

Figure 5b shows that even for a single device, multiple crossover points may exist depending on network conditions and the device's performance. For example, at 5 Mbps, TX2 processing in its top three performance modes outperforms offloading; however, as TX2's performance decreases beyond those modes, offloading becomes more advantageous. Across all scenarios, our models closely predict the crossover points, demonstrating their accuracy in capturing the tradeoff between the computation speedup of edge offloading and network delay.

Key takeaway. At high network bandwidths, edge offloading becomes favorable as its computational advantage outweighs the reduced network delays.

F. Impact of Collaborative Processing

To demonstrate our models' ability to capture collaborative (i.e., split) processing behavior, we consider an example using MobileNetV2 and use the Orin Nano as the device and A2 as

the edge under a 50 Mbps network. We evaluate three split points (SPs) where the model is progressively offloaded to the edge and compare them to full on-device execution. For each split point, the initial portion of the neural network is executed locally on the device, while the resulting intermediate output and remaining computation are offloaded to the edge. Figure 6a plots the observed latencies of each strategy alongside model predictions. To compute the end-to-end latency, we use the combined analytic models for device and edge processing as discussed in Section III-E. As shown, the latency increases with the amount of compute offloaded. This is because the intermediate results of later layers grow in size, adding to the network transfer overhead. As seen, for MobileNetV2 and the chosen network configuration, local processing is faster than split processing. Across all split points, the model-predicted latencies closely align with observed values. Note that other models will exhibit other types of behaviors with split processing, which we omit due to space constraints.

Key takeaway. Our models can be extended to capture both compute and network delays in device-edge collaborative processing.

G. Impact of Request Rate

Figure 6b shows how the request rate λ affects offloading decisions using the MobileNetV2 workload under 10 Mbps and 20 Mbps network bandwidth, with both the TX2 and Orin Nano set to their maximum performance modes. We observe two distinct behaviors depending on network bandwidth. At 10 Mbps, on-device processing using Orin Nano outperforms offloading across all RPS. However, at 20 Mbps, a performance crossover occurs: on-device processing is faster at low load ($RPS \leq 60$), while offloading becomes more efficient beyond that point. In contrast, processing on TX2 consistently exhibits higher latency across all RPS due to its limited performance. In all cases, as the system approaches saturation at high RPS, queue lengths show increased variability from the Poisson arrival process, leading to greater fluctuations in queuing delays and response times. Overall, the predicted end-to-end latencies of our models match closely with the observed latency within confidence intervals, demonstrating the accuracy of our models.

This result validates the competing scaling effects of λ discussed in Lemma III.1. Although both the network queuing

delays (for offloading) and local processing queuing delay (for on-device processing) grow with λ , the rate at which the delays increase differs depending on the hardware and network configurations. At 10 Mbps, the network queuing delay grows faster than the device queuing delay as λ increases, favoring on-device processing. Conversely, at 20 Mbps, device queuing delays become dominant at higher λ , shifting the advantage toward offloading.

Key takeaway. As load increases, on-device processing becomes more advantageous under slower networks, while offloading provides lower latency on faster networks.

H. Impact of Multi-Tenancy

We now experimentally validate the accuracy of our models in multi-tenant settings, using Orin Nano as the device and A2 as the edge server. We vary the number of applications deployed on the edge, each serving InceptionV4 requests, with all models loaded in memory concurrently. Each application receives 2 RPS from its corresponding client. We report the average offloading latency and compare it with on-device processing.

Figure 6c compares the average latency of offloading with on-device processing as the number of co-located applications increases. We observe that when only a single application is deployed on the edge, offloading yields lower latency than on-device processing. However, as the number of co-located applications increases, offloading latency also rises. This increase is caused by resource contention among applications because the A2 GPU does not support isolation. As a result, there is a crossover point at 18 applications, beyond which on-device processing becomes more efficient. Note that the on-device processing latency remains stable regardless of the number of concurrent applications as each device operates independently. In all cases, our models closely predict the latency for both execution strategies.

Key takeaway. Offloading latency increases with the number of co-located applications due to resource contention on edge servers lacking GPU isolation.

V. MODELS IN ACTION

In this section, we present a resource manager that leverages our analytic models to adaptively switch between offloading and on-device processing. We describe its decision algorithm and demonstrate its effectiveness through two case studies showcasing how the models enable adaptation to network variability and multi-tenant interference at the edge.

A. Model-Driven Adaptive Resource Management

The resource manager runs locally on the device and periodically collects runtime metrics, including network bandwidth, edge server load, and request arrival rate. At each epoch, it inputs these metrics into our models to estimate the average latency of both execution strategies and selects the one with the lower predicted latency to execute requests.

Algorithm 1 outlines the decision-making process for selecting the execution strategy. Lines 1-2 predict the on-device average execution latency based on the current arrival rate and

Algorithm 1: Model-Driven Adaptive Offloading

Input:

D_{req}, D_{res} : Request/result payload size
 $s_{dev}^{proc}, s_{edge}^{proc}$: Service times of device and edge
 λ_{dev} : Device task arrival rate
 B : Network bandwidth of device
 \mathcal{E} : Number of edge servers
 $\{\mu_{edge,E}^{proc}\}_{E=1}^{\mathcal{E}}$: Edge server aggregated service rates
 $\{\lambda_{edge,E}^{proc}\}_{E=1}^{\mathcal{E}}$: Edge server aggregated arrival rates

Output:

Execution strategy (on-device or edge server E^*)

```
// Predict on-device processing latency
1  $\mu_{dev}^{proc} \leftarrow 1/s_{dev}^{proc}$ 
2  $T_{dev} \leftarrow M/D/1(\lambda_{dev}^{proc}, \mu_{dev}^{proc}) + s_{dev}^{proc}$ 
// Predict edge offloading latency
3  $T_{net}^{req} \leftarrow M/M/1(\lambda_{dev}, B/D_{req}) + D_{req}/B$ 
4  $T_{net}^{res} \leftarrow M/M/1(\lambda_{edge,E}, B/D_{res}) + D_{res}/B$ 
5 for  $E \leftarrow 1$  to  $\mathcal{E}$  do
6    $T_{edge,E} \leftarrow T_{net}^{req} + M/G/1(\lambda_{edge,E}, \mu_{edge,E}^{proc}) + s_{edge}^{proc} + T_{net}^{res}$ 
// Select optimal strategy
7 if  $T_{dev} < \min(\{T_{edge,E}\}_{E=1}^{\mathcal{E}})$  then
8   return on_device_processing()
9 else
10   $E^* \leftarrow \arg \min_E T_{edge,E}$ 
11  return offload( $E^*$ ) // Offload to  $E^*$ 
```

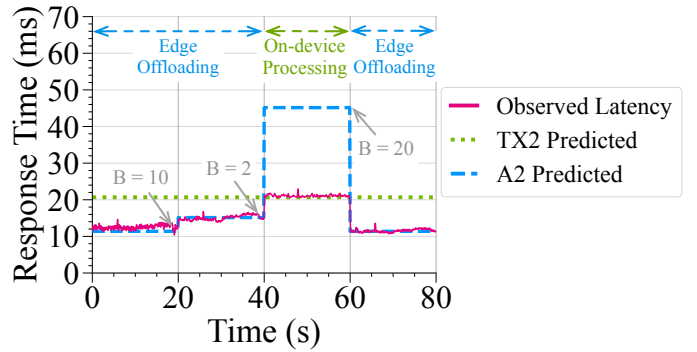


Fig. 7: Observed latency under changing network bandwidth as the resource manager selects between offloading and on-device processing. Bandwidth is varied at $t = 20, 40$, and 60 seconds.

the estimated service time on the device. Lines 3-6 compute the predicted average latency for offloading to each edge server, considering server load, service rates, and network conditions. Finally, Lines 7-11 execute the request using the strategy with the lower predicted latency.

B. Case 1: Fluctuating Network Conditions

We first demonstrate how the resource manager leverages our models to adapt to changing network conditions. We use TX2 as

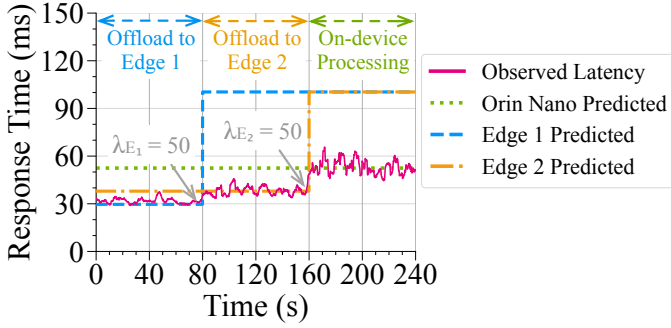


Fig. 8: Observed latency under varying edge server workloads. At $t = 80$, the request rate of edge server 1 is increased from 10 RPS to 50 RPS. At $t = 160$, the request rate of edge server 2 is also increased to 50 RPS.

the device, A2 as the edge, with MobileNetV2 requests arriving at a fixed rate of 10 RPS. Initially, the device has a network bandwidth of 20 Mbps to represent a stable 5G connection. To simulate real-world network variation, we reduce the bandwidth to 10 Mbps at $t = 20$ to reflect moderate signal degradation, further reduce it to 2 Mbps at $t = 40$ to emulate severe network congestion or poor coverage, and then restore it to 20 Mbps at $t = 60$ to represent signal recovery.

Figure 7 shows the observed latency using the execution strategies selected by the resource manager, alongside the model-predicted latencies for both offloading and on-device processing. At $t = 0$, the predicted offloading latency is lower than on-device processing, therefore the manager chooses to offload requests. At $t = 20$, despite the reduced bandwidth from 20 to 10 Mbps, the predicted latency for offloading remains lower, and the strategy remains unchanged. However, at $t = 40$, the drop to 2 Mbps causes the predicted offloading latency (45 ms) to exceed the predicted on-device processing time (21 ms), and the resource manager switches to on-device processing. Finally, at $t = 60$, as the network returns to 20 Mbps, the resource manager switches back to offloading. Throughout this sequence, the models closely predict the observed values, validating their accuracy.

Key takeaway. *Our models enable the resource manager to dynamically adapt to changing network conditions by switching between execution strategies.*

C. Case 2: Multi-tenant Edge Servers

Our second case study demonstrates how the resource manager leverages our models to adapt to workload changes across multiple multi-tenant edge servers. In this experiment, two edge servers, E_1 and E_2 , each equipped with an A2 GPU, are hosting separate instances of a YOLOv8n application. Initially, the request rates of each server are set to $\lambda_{E_1} = 10$ and $\lambda_{E_2} = 30$, while the TX2 running the resource manager has a request rate of $\lambda_{dev} = 10$. At $t = 80$, we add an additional device offloading request to E_1 to increase λ_{E_1} to 50. Similarly, at $t = 160$, we increase λ_{E_2} to 50.

Figure 8 shows the observed latencies alongside the predicted average latencies for offloading to E_1 , E_2 , and on-device

processing. Initially, from $t = 0$ to $t = 80$, the predicted latency for offloading to E_1 is the lowest, therefore the resource manager offloads requests to E_1 . However, at $t = 80$, as the workload on E_1 increases, its predicted latency rises. In response, the resource manager adapts by offloading to the less loaded server E_2 . At $t = 160$, as both servers reach a request rate of 50 RPS, the predicted latency for on-device processing becomes the lowest, and the resource manager shifts to on-device processing. This sequence highlights how our model enables the resource manager to dynamically adapt to fluctuations in edge server workload.

Key takeaway. *Our models enable the resource manager to dynamically adapt to workload changes in multi-tenant edge servers to maintain low latency.*

VI. RELATED WORK

Edge offloading. Edge offloading is a widely adopted strategy in many applications to enable resource-constrained devices to perform computationally intensive tasks by leveraging edge infrastructure [5], [8], [43], [44], [45], [6], [46], [47], [48], [49], [50], [51], [52]. For example, Furion [43] offloads computation-intensive components of mobile AR pipelines to the edge. Li et al. [44] introduce a hybrid chaotic evolutionary algorithm to dynamically determine the optimal offloading location of DNN layers under energy constraints. In contrast, our work uses a model-driven approach to reexamine whether offloading is advantageous in the era of accelerators. Our models apply to a wide range of workloads and generalizes to device-edge collaborative processing as shown in the evaluation.

Model-aware placement and resource allocation. Queuing models have been widely used to predict the performance of traditional CPU-bound workloads [53], [3], [54], [55], [56], [57], [20]. More recently, there has been growing interest in modeling the performance of hardware accelerators. For example, Merck et al. [58] model the latency of GPU batching in DNN inference workloads. Liang et al. [29] develop performance models for inference on accelerators (e.g., GPU, TPU) and use them to guide DNN placement via an online knapsack algorithm. In contrast, our models are applicable not only to inference workloads but also to other accelerator-driven applications as shown in Section IV-D. They jointly capture device hardware characteristics, network delays, and device-to-edge performance differences, enabling direct comparison between on-device processing and edge offloading.

Modeling distributed edge workloads. Several studies have developed analytic models for distributed device-edge-cloud environments. Raei et al. [59] analyze the impact of wireless signal strength on request rejection probability and mean response delay. FogQN [60] uses multi-class queuing networks to model fog and cloud computing to determine the optimal fraction of data processing executed at the cloud versus at fog servers. Loghin et al. [61] model MapReduce applications in hybrid edge-cloud environments. However, these works abstract away accelerator-specific queuing behavior and do not consider the effects of multi-tenancy at the edge. Our work complements existing efforts by addressing these missing dimensions through

a unified queuing-based modeling framework that informs resource management decisions.

VII. CONCLUSIONS

This paper presented analytic models to characterize the latency behavior of both on-device processing and edge offloading using hardware accelerators. We validated the accuracy of our model across a range of hardware, workloads, and network configurations. We developed a resource manager to demonstrate how model predictions can be used to dynamically adapt the execution strategy in response to changing network conditions and multi-tenant edge server workloads. As future work, we plan to extend the framework to model continuous batching in LLM inference and to support multi-stage pipelines or DAGs with dependencies across stages.

REFERENCES

- [1] E. Mosqueira-Rey, E. Hernández-Pereira, D. Alonso-Ríos, J. Bobes-Bascarán, and A. Fernández-Leal, "Human-in-the-loop machine learning: a state of the art," *Artif. Intell. Rev.*, vol. 56, p. 3005–3054, Aug. 2022.
- [2] A. Ali-Eldin, B. Wang, and P. Shenoy, "The hidden cost of the edge: a performance comparison of edge and cloud latencies," in *Proceedings of the International Conference for High Performance Computing, Networking, Storage and Analysis*, SC '21, (New York, NY, USA), Association for Computing Machinery, 2021.
- [3] B. Wang, D. Irwin, P. Shenoy, and D. Towsley, "Invar: Inversion aware resource provisioning and workload scheduling for edge computing," in *IEEE INFOCOM 2024 - IEEE Conference on Computer Communications*, (Vancouver, Canada), pp. 1511–1520, IEEE, 2024.
- [4] M. Satyanarayanan, P. Bahl, R. Caceres, and N. Davies, "The case for vm-based cloudlets in mobile computing," *IEEE Pervasive Computing*, vol. 8, no. 4, pp. 14–23, 2009.
- [5] A. Davis, J. Parikh, and W. E. Weihl, "Edgecomputing: extending enterprise applications to the edge of the internet," in *Proceedings of the 13th International World Wide Web Conference on Alternate Track Papers & Posters*, WWW Alt. '04, (New York, NY, USA), p. 180–187, Association for Computing Machinery, 2004.
- [6] J. Ren, Y. He, G. Huang, G. Yu, Y. Cai, and Z. Zhang, "An edge-computing based architecture for mobile augmented reality," *IEEE Network*, vol. 33, no. 4, pp. 162–169, 2019.
- [7] M. Satyanarayanan, G. Klas, M. Silva, and S. Mangiante, "The seminal role of edge-native applications," in *2019 IEEE International Conference on Edge Computing (EDGE)*, (Milan, Italy), pp. 33–40, IEEE, 2019.
- [8] S. Y. Jang, Y. Lee, B. Shin, and D. Lee, "Application-aware iot camera virtualization for video analytics edge computing," in *2018 IEEE/ACM Symposium on Edge Computing (SEC)*, (Seattle, WA, USA), pp. 132–144, IEEE, 2018.
- [9] Intel Corporation, "The ai pc powered by intel is here. now, ai is for everyone," 2025. Accessed: 2025-04-11.
- [10] T. Simonite, "Apple's neural engine infuses the iphone with ai smarts," Sep 2017.
- [11] Netatmo, "Smart outdoor camera." <https://shop.netatmo.com/en-us/security/cameras/camera-outdoor>, 2025. Accessed: 2025-04-11.
- [12] J. Huang, C. Samplawski, D. Ganesan, B. Marlin, and H. Kwon, "Clio: enabling automatic compilation of deep learning pipelines across iot and cloud," in *Proceedings of the 26th Annual International Conference on Mobile Computing and Networking*, MobiCom '20, (New York, NY, USA), Association for Computing Machinery, 2020.
- [13] Intel, "Intel movidius myriad x vpu." <https://www.movidius.com/myriadx/>, 2017. Accessed: 2024-08-19.
- [14] Google, "Edge tpu: Run inference at the edge." <https://cloud.google.com/edgetpu/>, 2019. Accessed: 2024-08-19.
- [15] NVIDIA, "Jetson tx2: High performance ai at the edge." <https://www.nvidia.com/en-us/autonomous-machines/embedded-systems/jetson-tx2/>, 2017. Accessed: 2024-08-19.
- [16] NVIDIA, "NVIDIA Jetson Orin Nano Developer Kit." <https://developer.nvidia.com/embedded/learn/get-started-jetson-orin-nano-devkit/>, 2023. Accessed: 2024-08-26.
- [17] NVIDIA, "Nvidia a2 tensor core gpu." <https://www.nvidia.com/en-us/data-center/products/a2/>, 2021. Accessed: 2025-04-10.
- [18] NVIDIA, "Multi-instance gpu (mig)." <https://www.nvidia.com/en-us/technologies/multi-instance-gpu/>, 2025. Accessed: 2025-04-11.
- [19] M. Harchol-Balter, *Performance Modeling and Design of Computer Systems: Queueing Theory in Action*. Cambridge University Press, 2013.
- [20] B. Urgaonkar, G. Pacifici, P. Shenoy, M. Spreitzer, and A. Tantawi, "An analytical model for multi-tier internet services and its applications," in *Proceedings of the 2005 ACM SIGMETRICS International Conference on Measurement and Modeling of Computer Systems*, SIGMETRICS '05, (New York, NY, USA), p. 291–302, Association for Computing Machinery, 2005.
- [21] NVIDIA, "Accelerated inference for large transformer models using nvidia fastertransformer and nvidia triton inference server." <https://github.com/NVIDIA/FasterTransformer/>, 2023. Accessed: 2025-06-10.
- [22] V. J. Reddi, C. Cheng, D. Kanter, P. Mattson, G. Schmuelling, C.-J. Wu, B. Anderson, M. Breughe, M. Charlebois, W. Chou, R. Chukka, C. Coleman, S. Davis, P. Deng, G. Diamos, J. Duke, D. Fick, J. S. Gardner, I. Hubara, S. Idgunji, T. B. Jablin, J. Jiao, T. S. John, P. Kanwar, D. Lee, J. Liao, A. Lokhmotov, F. Massa, P. Meng, P. Mickevicius, C. Osborne, G. Pekhimenko, A. T. R. Rajan, D. Sequeira, A. Sirasao, F. Sun, H. Tang, M. Thomson, F. Wei, E. Wu, L. Xu, K. Yamada, B. Yu, G. Yuan, A. Zhong, P. Zhang, and Y. Zhou, "Mlperf inference benchmark," in *Proceedings of the ACM/IEEE 47th Annual International Symposium on Computer Architecture*, ISCA '20, p. 446–459, IEEE Press, 2020.
- [23] NVIDIA, "NVIDIA System Management Interface (nvidia-smi)." <https://developer.nvidia.com/system-management-interface>, 2024. Accessed: 2024-04-13.
- [24] Z. Wang, P. Yang, B. Zhang, L. Hu, W. Lv, C. Lin, C. Zhang, and Q. Wang, "Performance prediction for deep learning models with pipeline inference strategy," *IEEE Internet of Things Journal*, vol. 11, no. 2, pp. 2964–2978, 2024.
- [25] S. Yao, Y. Zhao, H. Shao, S. Liu, D. Liu, L. Su, and T. Abdelzaher, "Fastdeepiot: Towards understanding and optimizing neural network execution time on mobile and embedded devices," in *Proceedings of the 16th ACM Conference on Embedded Networked Sensor Systems*, SenSys '18, (New York, NY, USA), p. 278–291, Association for Computing Machinery, 2018.
- [26] Y. Kang, J. Hauswald, C. Gao, A. Rovinski, T. Mudge, J. Mars, and L. Tang, "Neurosurgeon: Collaborative intelligence between the cloud and mobile edge," *SIGARCH Comput. Archit. News*, vol. 45, p. 615–629, apr 2017.
- [27] Y. Ji, D. Wei, L. Shi, P. Liu, C. Li, J. Yu, and X. Cai, "An active learning based latency prediction approach for neural network architecture," in *2024 4th International Conference on Neural Networks, Information and Communication Engineering (NNICE)*, pp. 967–971, 2024.
- [28] Z. Li, M. Paolieri, and L. Golubchik, "Predicting inference latency of neural architectures on mobile devices," in *Proceedings of the 2023 ACM/SPEC International Conference on Performance Engineering*, ICPE '23, (New York, NY, USA), p. 99–112, Association for Computing Machinery, 2023.
- [29] Q. Liang, W. A. Hanafy, A. Ali-Eldin, and P. Shenoy, "Model-driven cluster resource management for ai workloads in edge clouds," *ACM Trans. Auton. Adapt. Syst.*, vol. 18, Mar. 2023.
- [30] T. Amert, N. Otterness, M. Yang, J. H. Anderson, and F. D. Smith, "Gpu scheduling on the nvidia tx2: Hidden details revealed," in *2017 IEEE Real-Time Systems Symposium (RTSS)*, (Paris, France), pp. 104–115, IEEE, 2017.
- [31] A. Shah, R. Ganesan, S. Jajodia, and H. Cam, "A methodology to measure and monitor level of operational effectiveness of a csoc," *Int. J. Inf. Secur.*, vol. 17, p. 121–134, Apr. 2018.
- [32] A. Shah, R. Ganesan, S. Jajodia, P. Samarati, and H. Cam, "Adaptive alert management for balancing optimal performance among distributed csocs using reinforcement learning," *IEEE Trans. Parallel Distrib. Syst.*, vol. 31, p. 16–33, Jan. 2020.
- [33] D. Gross, J. F. Shortle, J. M. Thompson, and C. M. Harris, *Fundamentals of Queueing Theory*. USA: Wiley-Interscience, 4th ed., 2008.
- [34] M. Almeida, S. Laskaridis, S. I. Venieris, I. Leontiadis, and N. D. Lane, "Dyno: Dynamic onloading of deep neural networks from cloud to device," *ACM Trans. Embed. Comput. Syst.*, vol. 21, Oct. 2022.
- [35] A. Banitalebi-Dehkordi, N. Vedula, J. Pei, F. Xia, L. Wang, and Y. Zhang, "Auto-split: A general framework of collaborative edge-cloud ai," in *Proceedings of the 27th ACM SIGKDD Conference on*

- Knowledge Discovery & Data Mining, KDD '21*, (New York, NY, USA), p. 2543–2553, Association for Computing Machinery, 2021.
- [36] C. Hu, W. Bao, D. Wang, and F. Liu, “Dynamic adaptive dnn surgery for inference acceleration on the edge,” in *IEEE INFOCOM 2019 - IEEE Conference on Computer Communications*, (Paris, France), pp. 1423–1431, IEEE, 2019.
 - [37] E. Li, Z. Zhou, and X. Chen, “Edge intelligence: On-demand deep learning model co-inference with device-edge synergy,” in *Proceedings of the 2018 Workshop on Mobile Edge Communications, MECOMM'18*, (New York, NY, USA), p. 31–36, Association for Computing Machinery, 2018.
 - [38] S. Yang, Z. Zhang, C. Zhao, X. Song, S. Guo, and H. Li, “Cnnpc: End-edge-cloud collaborative cnn inference with joint model partition and compression,” *IEEE Transactions on Parallel and Distributed Systems*, vol. 33, no. 12, pp. 4039–4056, 2022.
 - [39] H. Pishro-Nik, *Introduction to Probability, Statistics, and Random Processes*. Springer, 2014.
 - [40] K. T. Marshall, “Some inequalities in queuing,” *Oper. Res.*, vol. 16, p. 651–668, June 1968.
 - [41] K. Gopalakrishnan, B. Hedayatnia, Q. Chen, A. Gottardi, S. Kwatra, A. Venkatesh, R. Gabriel, and D. Hakkani-Tur, “Topical-chat: Towards knowledge-grounded open-domain conversations,” 2023.
 - [42] The iPerf Project, “iperf - the tcp, udp, and sctp network bandwidth measurement tool,” 2025. Accessed: 2025-04-11.
 - [43] Z. Lai, Y. C. Hu, Y. Cui, L. Sun, and N. Dai, “Furion: Engineering high-quality immersive virtual reality on today’s mobile devices,” in *Proceedings of the 23rd Annual International Conference on Mobile Computing and Networking, MobiCom '17*, (New York, NY, USA), p. 409–421, Association for Computing Machinery, 2017.
 - [44] Z. Li, H. Yu, G. Fan, J. Zhang, and J. Xu, “Energy-efficient offloading for dnn-based applications in edge-cloud computing: A hybrid chaotic evolutionary approach,” *J. Parallel Distrib. Comput.*, vol. 187, May 2024.
 - [45] S. S. Ogden, X. Kong, and T. Guo, “Pieslicer: Dynamically improving response time for cloud-based cnn inference,” in *Proceedings of the ACM/SPEC International Conference on Performance Engineering, ICPE '21*, (New York, NY, USA), p. 249–256, Association for Computing Machinery, 2021.
 - [46] C. Mei, D. Taylor, C. Wang, A. Chandra, and J. Weissman, “Sharing-aware cloud-based mobile outsourcing,” in *2012 IEEE Fifth International Conference on Cloud Computing*, (Honolulu, HI, USA), pp. 408–415, IEEE, 2012.
 - [47] L. Liu, R. Zhong, W. Zhang, Y. Liu, J. Zhang, L. Zhang, and M. Gruteser, “Cutting the cord: Designing a high-quality untethered vr system with low latency remote rendering,” in *Proceedings of the 16th Annual International Conference on Mobile Systems, Applications, and Services, MobiSys '18*, (New York, NY, USA), p. 68–80, Association for Computing Machinery, 2018.
 - [48] Z. Chen, W. Hu, J. Wang, S. Zhao, B. Amos, G. Wu, K. Ha, K. Elgazzar, P. Pillai, R. Klatzky, D. Siewiorek, and M. Satyanarayanan, “An empirical study of latency in an emerging class of edge computing applications for wearable cognitive assistance,” in *Proceedings of the Second ACM/IEEE Symposium on Edge Computing, SEC '17*, (New York, NY, USA), Association for Computing Machinery, 2017.
 - [49] J. Wang, Z. Feng, Z. Chen, S. George, M. Bala, P. Pillai, S.-W. Yang, and M. Satyanarayanan, “Bandwidth-efficient live video analytics for drones via edge computing,” in *2018 IEEE/ACM Symposium on Edge Computing (SEC)*, (Seattle, WA, USA), pp. 159–173, IEEE, 2018.
 - [50] Z. Zhang, X. Lin, G. Xue, Y. Zhang, and K. S. Chan, “Joint optimization of task offloading and resource allocation in tactical edge networks,” in *MILCOM 2024 - 2024 IEEE Military Communications Conference (MILCOM)*, (Washington, DC, USA), pp. 703–708, IEEE, 2024.
 - [51] O. Tkachenko, S. Harding, C. Anderson, J. Perazzone, M. Dwyer, and K. Chan, “Characterizing the performance of distributed edge processing resource allocation in dynamic networked environments,” in *MILCOM 2023 - 2023 IEEE Military Communications Conference (MILCOM)*, (Boston, MA, USA), pp. 888–893, IEEE, 2023.
 - [52] S. S. Ogden and T. Guo, “Layercake: Efficient inference serving with cloud and mobile resources,” in *2023 IEEE/ACM 23rd International Symposium on Cluster, Cloud and Internet Computing (CCGrid)*, (Bangalore, India), pp. 191–202, IEEE, 2023.
 - [53] L. Jiang, X. Chang, J. Mišić, V. Misić, and R. Yang, “Performance analysis of heterogeneous cloud-edge services: A modeling approach,” *Peer-to-Peer Networking and Applications*, vol. 14, 01 2021.
 - [54] A. N. Tantawi and D. Towsley, “Optimal static load balancing in distributed computer systems,” *J. ACM*, vol. 32, p. 445–465, Apr. 1985.
 - [55] P. Ambati, N. Bashir, D. Irwin, and P. Shenoy, “Waiting game: Optimally provisioning fixed resources for cloud-enabled schedulers,” in *SC20: International Conference for High Performance Computing, Networking, Storage and Analysis*, (Atlanta, GA, USA), pp. 1–14, IEEE, 2020.
 - [56] A. Gandhi and A. Suresh, “Leveraging queueing theory and os profiling to reduce application latency,” in *Proceedings of the 20th International Middleware Conference Tutorials, Middleware '19*, (New York, NY, USA), p. 1–5, Association for Computing Machinery, 2019.
 - [57] Z. Shen, S. Subbiah, X. Gu, and J. Wilkes, “Cloudscale: elastic resource scaling for multi-tenant cloud systems,” in *Proceedings of the 2nd ACM Symposium on Cloud Computing, SOCC '11*, (New York, NY, USA), Association for Computing Machinery, 2011.
 - [58] M. L. Merck, B. Wang, L. Liu, C. Jia, A. Siqueira, Q. Huang, A. Saraha, D. Lim, J. Cao, R. Hadidi, and H. Kim, “Characterizing the execution of deep neural networks on collaborative robots and edge devices,” in *Practice and Experience in Advanced Research Computing 2019: Rise of the Machines (Learning)*, PEARC '19, (New York, NY, USA), Association for Computing Machinery, 2019.
 - [59] H. Raei, N. Yazdani, and R. Shojaei, “Modeling and performance analysis of cloudlet in mobile cloud computing,” *Performance Evaluation*, vol. 107, pp. 34–53, 2017.
 - [60] U. Tadakamalla and D. Menascé, “Fogqn: An analytic model for fog/cloud computing,” in *2018 IEEE/ACM International Conference on Utility and Cloud Computing Companion (UCC Companion)*, pp. 307–313, 2018.
 - [61] D. Loghin, L. Ramapantulu, and Y. M. Teo, “Towards analyzing the performance of hybrid edge-cloud processing,” in *2019 IEEE International Conference on Edge Computing (EDGE)*, pp. 87–94, 2019.